

Article

Optimal Stator Design of Doubly Salient Permanent Magnet Generator for Enhancing the Electromagnetic Performance

Vannakone Lounthavong, Warat Sriwannarat, Apirat Siritaratiwat and Pirat Khunkitti * 

Department of Electrical Engineering, Faculty of Engineering, Khon Kaen University, Khon Kaen 40002, Thailand

* Correspondence: piratkh@kku.ac.th; Tel.: +66-86-636-5678

Received: 10 July 2019; Accepted: 19 August 2019; Published: 20 August 2019



Abstract: An optimal stator design technique of a three-phase doubly salient permanent magnet generator (DSPMG) for improving the output power is proposed. The stator configuration was optimally designed by adjusting the stator pole depth and stator pole arc. The trapezoid outer stator tip was also designed. Then, the output characteristics of the designed DSPMG including the flux linkage, electromotive force (EMF), harmonic, cogging torque, efficiency, magnetic flux distribution and voltage regulation were characterized by using the finite element method. Results were compared to the original structure in the literature. It was found that the flux linkage, EMF, cogging torque, and efficiency of the proposed DSPMG were significantly improved after the stator pole depth and stator pole arc were suitably modified. Further details of optimal stator pole depth and stator pole arc are presented. The EMF produced by the optimal proposed structure was 47% higher than that of the conventional structure, while 56% cogging torque improvement and 20% increased efficiency were achieved. The EMF generated by the proposed structure was classified in the high-range scale compared to the other existing models. The symmetrical magnetic flux distribution of all structures was indicated. The voltage regulation of the modified structure was also significantly improved from the conventional model. The proposed design technique can be utilized to maximize the electromagnetic performance of this particular generator type.

Keywords: permanent magnet machine; doubly salient permanent magnet generator; magnetic flux linkage; electromotive force; voltage regulation

1. Introduction

Currently, the use of renewable energy resources attracts worldwide attention for electrical generation since it successfully relieves the energy crisis and environmental deterioration. In order to efficiently produce electricity, high-efficiency machines are desired. Permanent magnet (PM) machines are extensively utilized as electrical generators in renewable applications, such as hydro and wind energies, due mainly to their outstanding advantages, for instance, high power density, high torque density, high reliability, and freedom from excitation loss [1,2]. These machines can be categorized into two types, namely, the stator permanent magnet machine and the rotor permanent magnet machine, depending on the location of the installed PM [3]. The rotor PM machines comprise a PM mounted at the rotor structure, and these machines are suitable for operating in low-speed applications [4,5]. The stator PM machines contain a PM and winding at the stator; as a result, the rotor of these machines has low weight and inertia [6]. Several stator PM machines exist in the literature, e.g., flux-reversal PM machines [7,8], the switch-flux PM machines [9,10], and doubly salient permanent magnet (DSPMG) machines [11–13].

In particular, several studies claimed that the DSPM machines are highly appropriate for low-speed applications due to their many advantages over other stator PM machines, for instance, higher efficiency, higher power density, higher power output, and lower inertia and ripple torque [14–16]. Later on, the DSPM machines were developed for use as electrical generators, known as doubly salient permanent magnet generators (DSPMGs) [17–19]. The outstanding points of DSPMG were extensively reported [18–21]. In addition, a novel three-phase DSPMG was proposed by Zhang et al.; it was indicated that the DSPMG with a 12/8 (stator/rotor) pole could produce high output power [22]. However, we remarked that the performance of this generator can be further improved by optimizing the stator configuration since this structural parameter is strongly related to the machine performance.

Thus, this paper purposes an optimal stator design technique for improving the electromagnetic performance of the DSPMG. The structural parameters of stator pole configuration including the stator pole depth and stator pole arc were optimized. The characteristics of the DSPMG comprising the flux linkage, electromotive force (EMF), harmonic, cogging torque, efficiency, magnetic flux distribution, and voltage regulation profiles were investigated. The simulations were based on a two-dimensional finite element method (2D-FEM).

2. Machine Design

2.1. Magnetic Field Distribution Analysis

The conventional structure of the DSPMG used in this work was initially designed by Zhang et al., as illustrated in Figure 1a [22]. The regular model consists of 12 inner stator poles and eight outer rotor poles, written as 12/8 stator/rotor poles. The stator and rotor poles are salient poles. The winding is inserted at the stator slot opening. Four pieces of an Nd–Fe–B permanent magnet are inserted at the stator yoke for supplying field excitation. Since the permanent magnets and armature windings are assembled at the stator, the rotor of this structure has a very low weight. The detail of the parameters of the DSPMG are illustrated in Table 1. The stator pole depth and stator pole arc are adjusted in order to evaluate the optimal value of those parameters. Figure 1b demonstrates the proposed optimal DSPMG model in this work; further design details and information are provided in Section 3.

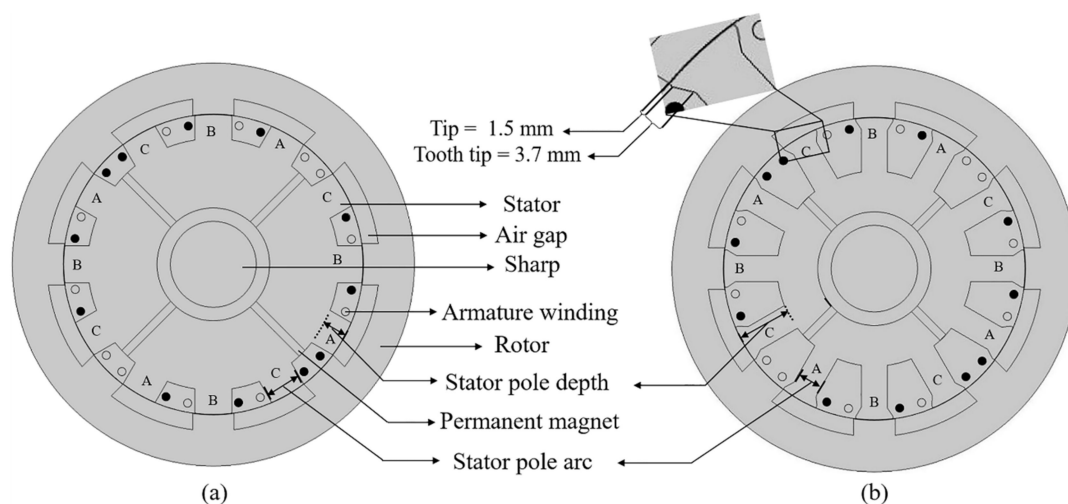


Figure 1. Cross-sectional perspective of the 12/8 stator/rotor pole doubly salient permanent magnet generator (DSPMG): (a) conventional model [22]; (b) proposed optimal model.

Table 1. The structural parameters of the 12/8 stator/rotor pole conventional doubly salient permanent magnet generator (DSPMG) [22].

Parameters of Conventional DSPMG	Value
Stator pole number	12
Rotor pole number	8
Outer diameter of rotor (mm)	150
Inner diameter of rotor (mm)	118
Air gap length (mm)	0.45
Inner diameter of stator (mm)	42
Stator pole depth (mm)	18
Rotor pole depth (mm)	6
Stack length (mm)	22
Stator pole arc (°)	13.5
Rotor pole arc (°)	15
Number of turns/phases	344
Permanent magnet number	4
Permanent magnet thickness (mm)	6
Cross-section area of winding coil (mm ²)	0.56
Rated speed (rpm)	3600

2.2. Analysis of Machine Characteristics

In the analysis of machine characteristics, 2D-FEM was performed in the calculations by using COMSOL software (version 4.2, Khon Kaen University, Khon Kaen, Thailand). The flux linkage and EMF profiles of the generator were evaluated as shown in the equations below. Firstly, the magnetic vector potential in the z -axis, A_z , was obtained by Ampere's law, shown in Equation (1).

$$\sigma \frac{\partial A_z}{\partial t} + \left(\frac{1}{\mu_0} (\Delta \times A_z - B_r) \right) = J_e \quad (1)$$

where B_r is the remanent flux density of the Nd-Fe-B permanent magnet (1.08 T), J_e is the external generated current density (0 A), μ_0 is the vacuum permeability of air, and σ is the electrical conductivity of air. The electric field in the z -direction, E_z , is calculated by substituting A_z into Faraday's law, as shown in Equation (2).

$$\nabla \times E_z = \frac{-\sigma (\nabla \times A_z)}{\partial t} \quad (2)$$

The flux linkage, $\psi_{linkage}$, existing in the machine structure can be calculated using Equation (3).

$$\psi_{linkage} = N \times \frac{L}{A} \int A_z dA \quad (3)$$

where N is the number of turns of the winding coil, L is the stack length in the z -axis, and A is the area of the winding cross-section. Then, the magnitude of EMF can be obtained using Equation (4).

$$EMF = N \frac{L}{A} \int E_z dA \quad (4)$$

In order to improve the electromagnetic performance of the generator, the optimal values of stator pole depth and stator pole arc of the conventional DSPMG were determined based on a consideration of the magnetic flux linkage, EMF, harmonic, cogging torque, efficiency, magnetic flux distribution, and voltage regulation profiles. Since these structural parameters are directly related to the area of the winding coil, it should be noted that the number of winding turns after adjusting the stator configuration was taken into account.

3. Results and Discussion

3.1. Influence of Stator Pole Depth on the Generator Outputs

In this sub-section, the influence of stator pole depth on the magnetic flux linkage and EMF profiles of the DSPMG is investigated. The range of stator pole depth was varied from 18 mm to 43.2 mm, which represents 100% to 240% of the conventional value. Once the stator pole depth was increased, an available area for inserting the armature winding practically became larger. Table 2 demonstrates the number of winding turns at various stator pole depths. It is shown that a winding coil with 44 turns can be additionally installed when the stator pole depth is increased by 20%. Figure 2a shows the flux linkage profile of the proposed DSPMG with different stator pole depths, while the maximum value of flux linkage is illustrated in Figure 2b. The pattern of the flux linkage waveform at all stator pole depths looks similar. From Figure 2b, it is indicated that the flux linkage increased upon increasing the stator pole depth and reached the maximum value at 36 mm of stator pole depth. Afterward, the flux linkage decreased. The characteristic of EMF produced by the proposed DSPMG is illustrated in Figure 3a, whereas the maximum EMF is shown in Figure 3b. From Figure 3a, the EMF waveform at all stator pole depths exhibits a good pattern and is acceptable. Also, it was found that higher magnitudes of EMF were reached upon increasing the stator pole depth. The maximum EMF of 344.92 V was found at 39.6 mm of stator pole depth; afterward, the EMF steadily reduced. As shown in Figure 3c, the harmonic profile indicates that this machine has no even harmonics due to a symmetrical EMF waveform. However, the odd harmonics were present due to the small oscillation of the EMF profile, which may accordingly cause a ripple to the generator output. The DSPMG structure with a shorter stator pole depth seemed to have a better harmonic scale; however, the various harmonic scales were acceptable.

Table 2. Relationship between stator pole depth and number of winding turns.

Percentage of Stator Pole Depth Compared to Original Configuration (%)	Stator Pole Depth (mm)	Winding Turn (Turn)
100	18	344
120	21.6	388
140	25.2	432
160	28.8	476
180	32.4	520
200	36	564
220	39.6	608
240	43.2	652

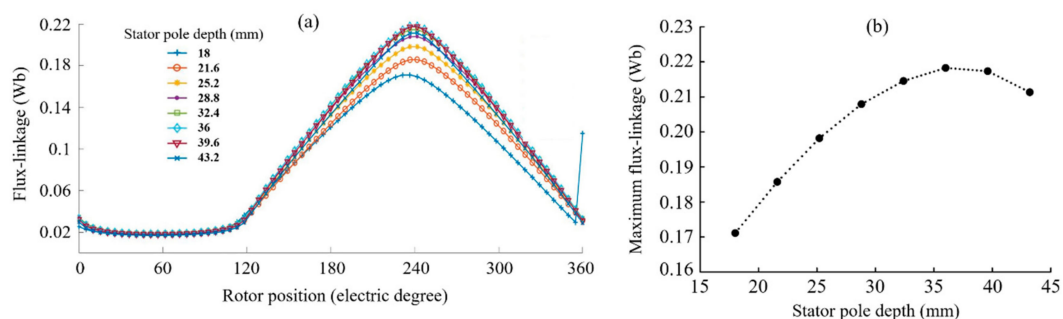


Figure 2. The characteristic of magnetic flux linkage with varying stator pole depths: (a) the waveform at each rotor position; (b) the maximum value.

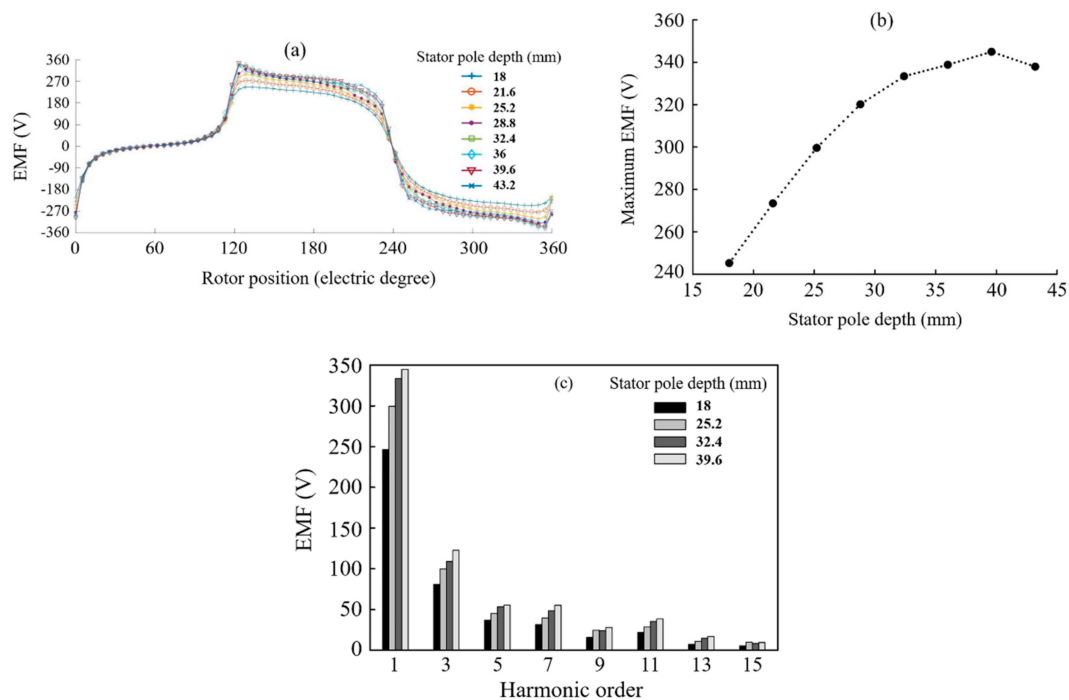


Figure 3. The characteristic of electromotive force (EMF) with varying stator pole depths: (a) the waveform at each rotor position; (b) the maximum value; (c) the spectrum.

The physical explanation regarding the change in flux linkage and EMF with varying stator pole depths is detailed as follows: once the stator pole depth was increased, the length of PM decreased while the winding area became larger. Although shorter PM lengths typically supplied a lower flux linkage to the armature winding, the increase in the number of winding turns totally compensated for the lack of flux linkage. Then, the flux-linkage could be increased for deeper stator poles. This compensation also happened for the EMF profile. However, the flux linkage and the EMF became smaller when the stator pole depth was reduced by more than 36 and 39.6 mm, respectively. This was because, when the stator pole depth was beyond these points, the magnetic field strength from the PM was too weak to be transmitted through the machine structure. As a result, the flux linkage was inadequate to produce EMF. Thus, the number of winding turns indicated a stronger influence on the flux linkage and EMF than the length of the PM for only a particular range of stator pole depths.

Figure 4 demonstrate the cogging torque waveforms of the DSPMG with stator pole depths of 18, 25.2, 32.4, and 39.6 mm. A symmetrical property of the cogging torque profile was well indicated for all structures. It is shown that the cogging torque linearly improved upon increasing the stator pole depth from 18 m to 39.6 mm. From the results, it was obviously found that the cogging torque was reduced upon increasing stator pole depth because an increase in stator pole depth resulted in a shortening of the distance between the PMs and the rotor structure, as well as a reduction in the magnetic field generated from the PMs due to smaller PM volumes. Thus, the DSPMG with a stator pole depth of 39.6 nm was indicated as the most suitable torque in starting conditions, whereby the torque amplitude was about 56.17% smaller than the conventional scale.

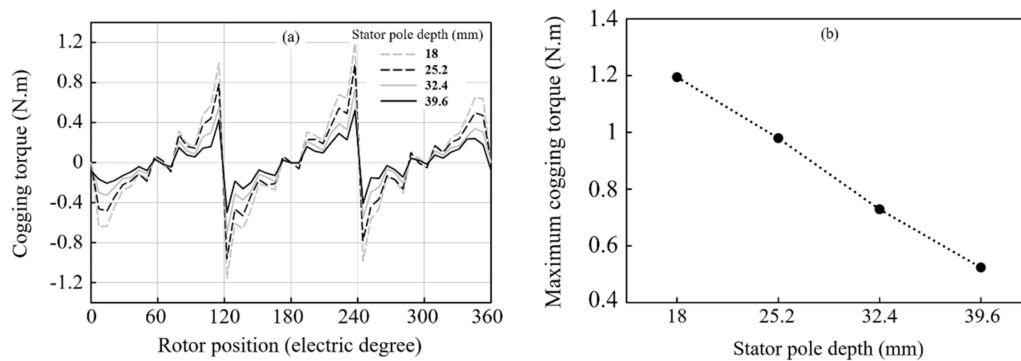


Figure 4. (a) Cogging torque waveform of the DSPMG with varying stator pole depths; (b) the maximum value.

The efficiency of the DSPMG with stator pole depths of 18, 25.2, 32.4, and 39.6 mm is shown in Figure 5. An input power of 200 W and a constant load current of 0.2 A were assumed in the calculation. It was found that the DSPMG with a stator pole of depth 32.4 mm demonstrated the highest efficiency, followed by depths of 39.6, 25.2, and 18 mm. An improvement in generator efficiency upon lengthening the stator pole depth from 18 to 32.4 was due to an increase of EMF magnitude. After that, the efficiency was slightly decreased due to an excessive number of winding coils. Generator efficiency of up to 97.37% can be achieved by adjusting the stator pole depth to 32.4 mm. However, when considering the results of the EMF and cogging torque concurrently with efficiency, the stator pole depth of 39.6 mm indicated the most suitable output profile. Although the efficiency of the DSPMG with a stator pole depth of 39.6 mm was slightly less than that of 32.4 mm, it demonstrated the highest EMF and smallest cogging torque value. The DSPMG with optimal stator pole depth could produce 40% higher EMF and 17% better efficiency than the conventional structure. This optimum stator pole depth value was selected to further examine the generator output upon varying the stator pole arc in the following sub-section.

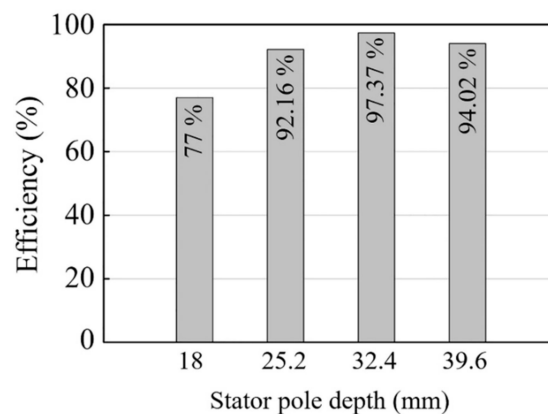


Figure 5. Efficiency of the DSPMG at various stator pole depths.

3.2. Influence of Stator Pole Arc on the Generator Outputs

In this sub-section, the effects of stator pole arc adjustment on the flux linkage and EMF of the proposed DSPMG are examined. The optimal stator pole depth of 39.6 mm was fixed in this evaluation. The stator pole arc of the DSPMG was adjusted from 13.5 degrees to 8.1 degrees, which represents 100% to 60% of the conventional angle. While reducing the stator pole arc, we designed a trapezoid outer stator tip based on an original stator tip arc in order to efficiently provide a good leading of the magnetic flux linkage through the machine structure. An example of the DSPMG with a trapezoid stator tip was previously illustrated in Figure 1b. Once the stator pole arc was reduced, the area for inserting the armature winding at the stator slot opening practically became larger. As a result, the number of

winding turns could be increased. Table 3 shows the relationship between the stator pole arc and the number of installed winding turns. It can be seen that winding coils could be additionally inserted when the stator pole arc was reduced. The characteristics of generator output including the flux linkage and EMF for various stator pole arcs are shown in Figures 6 and 7, respectively. It was found that the flux linkage rapidly increased when the stator pole arc was reduced from 13.5 to 12.15 degrees. After that, it decreased with a reduction in stator pole arc. Meanwhile, the EMF continually increased when the stator pole arc became narrower. From the harmonic waveforms shown in Figure 7c, only odd harmonics were present due to a symmetrical EMF waveform at all stator pole arcs. The wider stator pole arc seemed to have the worst harmonic profile for only the third order but quite good for the rest. The harmonic profile of the DSPMG with a stator pole arc of 12.15 degrees was average compared to the other stator pole arcs. Only a slight difference in harmonic was detected above the third order.

Table 3. Relationship between stator pole arc and number of winding turns at a stator pole depth of 39.6 mm.

Percentage of Stator Pole Arc Compared to Original Configuration (%)	Stator Pole Arc (Degree)	Winding Turns (Turn)
100	13.50	608
95	12.83	622
90	12.15	636
85	11.48	648
80	10.80	662
75	10.13	674
70	9.45	686
65	8.78	696
60	8.10	708

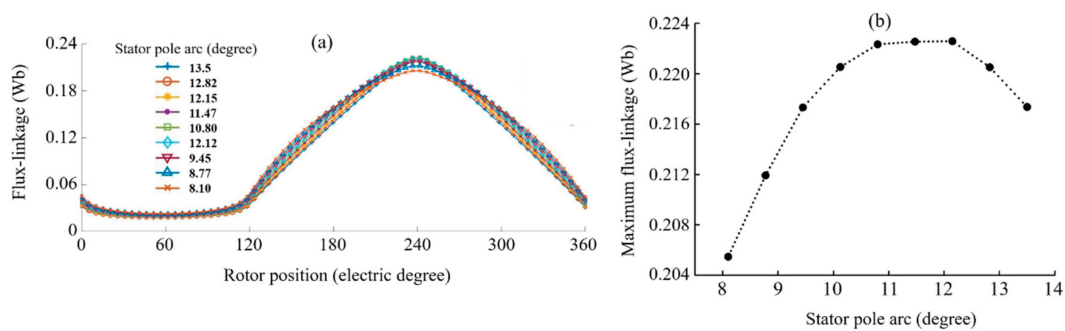


Figure 6. The characteristic of magnetic flux linkage with varying stator pole arcs: (a) the waveform at each rotor position; (b) the maximum value.

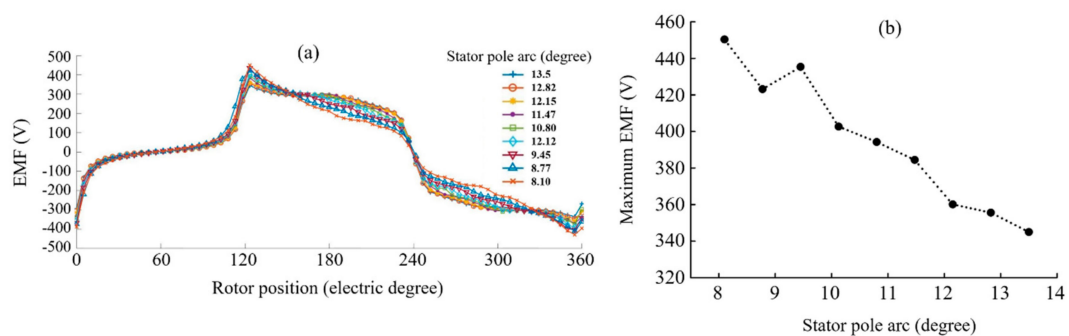


Figure 7. Cont.

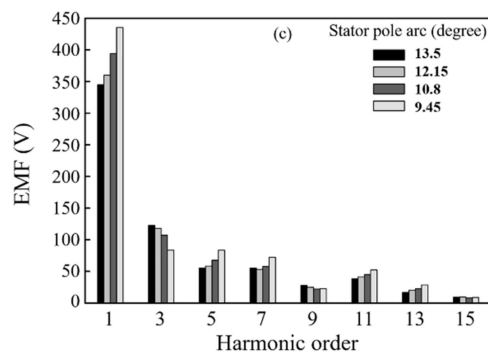


Figure 7. The characteristic of EMF with varying stator pole arcs: (a) the waveform at each rotor position; (b) the maximum value; (c) the spectrum.

Upon reducing the stator pole arc from 13.5 to 12.15 degrees, the flux linkage became larger due to the influence of additional winding turns. Thus, the flux linkage rapidly decreased for narrower pole arcs due to the existence of flux leakage; this was because the stator pole was too narrow to contain the magnetic field. The higher EMF produced by the generator for narrower stator pole arcs resulted from the effect of additional winding turns. However, it was obviously found that the stator pole arc not only had an impact on the magnitude of the flux linkage and EMF, but also caused a fluctuation in the EMF waveform. As can be seen from Figure 5a, although the maximum magnitude of EMF increased for narrower stator pole arcs, the waveform of EMF became increasingly unstable. We found that the EMF waveform was unsuitable for use in generator applications when the stator pole arc was narrower than 70% of the initial value.

Figure 8 demonstrates the cogging torque waveforms of the DSPMG with stator pole arcs of 13.5, 12.15, 10.8, and 9.45 mm. A symmetrical property of the cogging torque profile was well indicated for all structures. The result showed that the cogging torque was improved upon reducing the pole arc from 13.5 to 12.15; afterward, it became worse for smaller pole arcs. An increase in cogging torque for narrower stator pole arcs occurred because the narrower stator teeth contained much higher magnetic flux densities flowing through the stator teeth toward the air gap. As a result, the cogging torque became larger due to higher magnetic flux densities at the air gap. However, an increase in magnetic flux density had a slight effect on the initial pole arc range, as can be seen from the cogging torque profile for stator pole arcs of 13.5 and 12.15 degrees. Remarkably, it was noticed that the cogging torque decreased upon reducing the stator pole arc from 13.5 to 12.15 mm, whereas the EMF was significantly improved by this stator pole arc alteration. Thus, the DSPMG with a stator pole arc of 12.15 mm could produce the most appropriate cogging torque profile; the cogging torque produced from this structure was 56.5% smaller than the conventional structure.

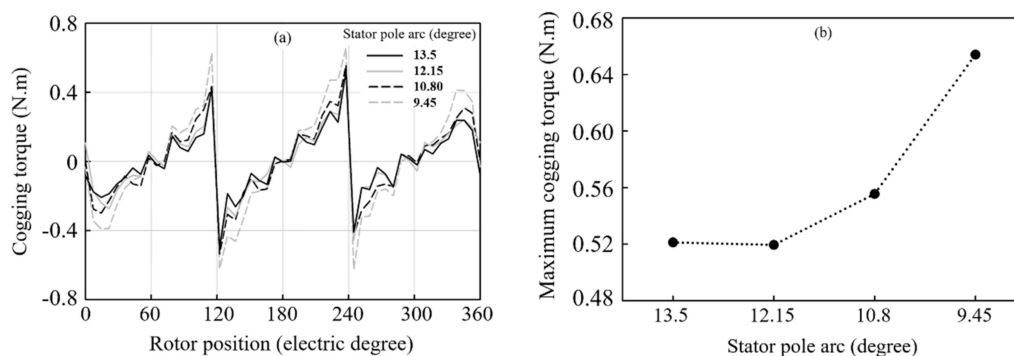


Figure 8. (a) Cogging torque waveform of the DSPMG with varying stator pole arcs; (b) the maximum value.

The efficiency of the DSPMG with stator pole arcs of 13.50, 12.15, 10.80, and 9.45 degrees is shown in Figure 9. An input power of 200 W and a constant load current of 0.2 A were assumed in the calculation. It was found that the DSPMG with a stator pole of arc 12.15 mm demonstrated the highest efficiency up to 96.76%, followed by 13.5, 10.8, and 9.45 mm. The reason that the stator pole arc of 12.15 mm could produce the highest efficiency was because the generator efficiency dominantly depended on the EMF magnitude in the initial pole arc range. After that, the efficiency was reduced due to an excessive number of winding coils.

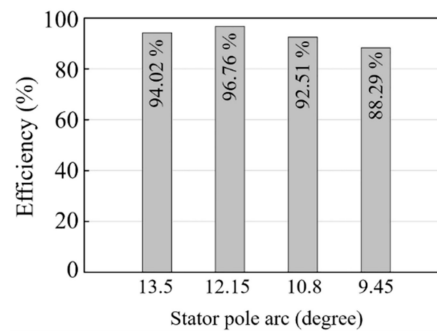


Figure 9. Efficiency of the DSPMG for various stator pole arcs.

From the results, the stator pole arc of 12.15 degrees was chosen as a suitable configuration for the proposed DSPMG. At this point, the flux linkage of the structure reached the maximum value, which implies that the magnetic flux could greatly flow through the machine structure. Although the maximum EMF at this point was less than that of narrower pole arcs, the waveform of the EMF was pretty symmetric. The DSPMG with a stator pole arc of 12.15 degrees demonstrated the best cogging torque profile and highest efficiency. More importantly, the stator pole arc is practically used as a winding core thus, reducing the stator pole arc may decrease the robustness of the stator pole. Therefore, it should not be too narrow. From the findings, the maximum EMF produced by the proposed DSPMG with a suitable stator pole depth and stator pole arc was 360 V, which was 47% higher than that of the conventional structure; moreover, 56.5% smaller cogging torque and a 20% improvement in efficiency could be achieved. The EMF produced by this optimal proposed structure can be classified in the high-range scale compared to the other existing models of this particular generator type. The results can be utilized to design the optimal stator structure of the DSPMG.

3.3. Magnetic Flux Distribution Analysis

The magnetic flux distribution of the selected DSPMG structures at no-load conditions was analyzed. Figure 10a–c show the magnetic flux distribution of the conventional DSPMG, the DSPMG structure with optimized stator pole depth, and the DSPMG structure with optimized stator pole depth and stator pole arc, respectively. It was confirmed that the magnetic flux distribution flowing through the generator structure was greatly symmetric for all structures. The symmetrical magnetic flux results in symmetrical flux linkage circulation, as previously indicated in Figures 2a and 6a.

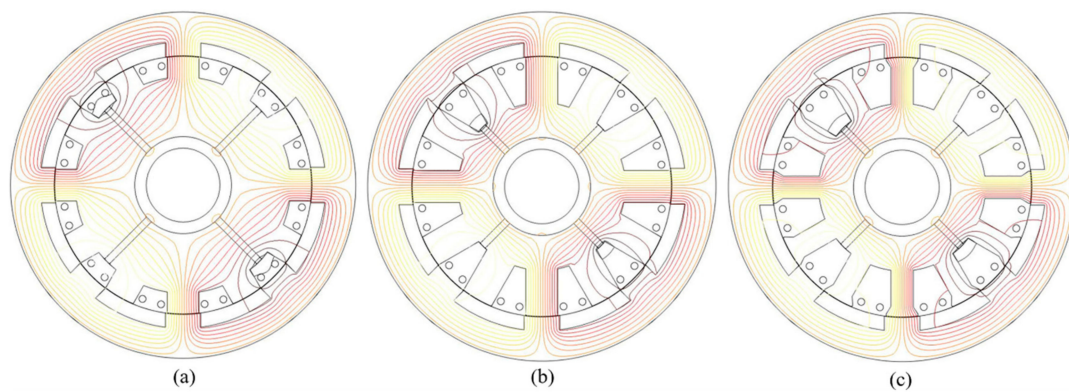


Figure 10. The magnetic flux distribution at no-load conditions for the DSPMG with (a) the conventional structure, (b) the structure with optimized stator pole depth, and (c) the structure with optimized stator pole depth and stator pole arc.

3.4. Voltage Regulation Analysis

Figure 11 shows the voltage regulation under load conditions of the selected DSPMG structures including the conventional DSPMG, the DSPMG structure with optimized stator pole depth, and the DSPMG structure with optimized stator pole depth and stator pole arc. The winding coil of the conventional structure included 344 turns, the DSPMG structure with optimized stator pole depth included 608 turns, and the DSPMG structure with optimized stator pole depth and stator pole arc included 636 turns. The voltage regulation was demonstrated through the phase voltage magnitude at various load currents. It can be seen that the proposed optimal structure provided significantly improved voltage regulation compared to the conventional structure. The structure with optimized stator pole depth and stator pole arc indicated better voltage regulation than the others, which implies that this optimized structure could produce higher output power and can be widely utilized in several applications.

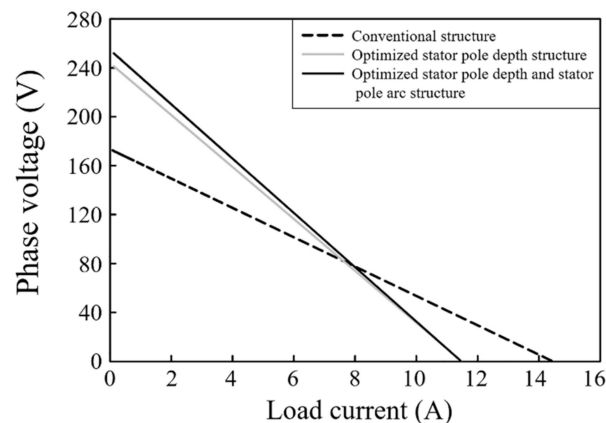


Figure 11. The voltage regulation of each DSPMG structure.

In the real design of a DSPMG, one needs to be aware of any geometrical tolerances during the manufacturing process since they directly influence the magnetic flux path. It should be noted that the most sensitive portion of the magnetic path is the airgap. The tolerance of the airgap could essentially cause errors in generator performance indicators such as magnetic flux linkage, EMF, cogging torque, efficiency, and voltage regulation; it might also cause an increase in leakage flux in the structure.

4. Conclusions

In this work, the optimal stator configuration of a DSPMG was designed by adjusting the stator pole depth and stator pole arc in order to improve the electromagnetic performance of the generator.

The output characteristics of the proposed generator including magnetic flux linkage, EMF, harmonic, cogging torque, efficiency, magnetic flux distribution, and voltage regulation were examined using the finite element method. The results showed that the flux linkage and EMF of the DSPMG were significantly improved when the stator pole depth and stator pole arc were appropriately adjusted, while a good spectrum of EMF waveforms was also demonstrated. The stator pole depth of 39.6 mm indicated the most suitable flux linkage and EMF profiles. Meanwhile, the stator pole arc of 12.15 degrees based on a modified trapezoid stator tip was chosen as the optimal pole arc. The optimum structure of the DSPMG could produce an EMF of up to 360 V, which is about 47% higher than that of the original structure; moreover, 56% cogging torque enhancement and a 20% improvement in efficiency were achieved. The symmetrical property of the magnetic flux distribution was additionally demonstrated. Moreover, the optimum proposed structure indicated significantly improved voltage regulation, which implies that this optimal structure can produce higher output power, as well as electromagnetic performance, compared to the conventional structure. This optimizing technique can be utilized to design DSPM generators which are widely researched in the current literature.

Author Contributions: Conceptualization, V.L. and P.K.; methodology, V.L. and P.K.; software, V.L.; validation, V.L. and P.K.; formal analysis, V.L., W.S., A.S., and P.K.; investigation, P.K.; resources, P.K.; data curation, V.L.; writing—original draft preparation, V.L.; writing—review and editing, P.K.; visualization, V.L., W.S., A.S., and P.K.; supervision, P.K.; project administration, P.K.; funding acquisition, V.L. and P.K.

Funding: This research was funded by the Electricity Generating Authority of Thailand (EGAT), Electricite du Laos (EDL), EDL–Generation public company (EDL–GEN). This work was also financially supported by the Thailand Research Fund (grant numbers MRG6180010).

Acknowledgments: The authors would also like to thank the Department of Mechanical Engineering, Khon Kaen University for access to the COMSOL software.

Conflicts of Interest: The authors declare no conflicts of interest.

References

1. Wang, Y.; Niu, S.; Fu, W. Electromagnetic Performance Analysis of Novel Flux-Regulatable Permanent Magnet Machines for Wide Constant-Power Speed Range Operation. *Energies* **2015**, *8*, 13971–13984. [[CrossRef](#)]
2. Chau, K.T.; Chan, C.C.; Liu, C. Overview of permanent-magnet brushless drives for electric and hybrid electric vehicles. *IEEE Trans. Ind. Electron.* **2008**, *6*, 2246–2257. [[CrossRef](#)]
3. Cheng, M.; Hua, W.; Zhang, J.; Zhao, W. Overview of stator-permanent magnet brushless machines. *IEEE Trans. Ind. Electron.* **2011**, *58*, 5087–5101. [[CrossRef](#)]
4. Ko, H.S.; Kim, K.J. Characterization of noise and vibration sources in interior permanent-magnet brushless DC motors. *IEEE Trans. Magn.* **2004**, *6*, 3482–3489. [[CrossRef](#)]
5. Gieras, J.F.; Wang, R.J.; Kamper, M.J. *Axial Flux Permanent Magnet Brushless Machines*, 2nd ed.; Springer-Verlag: New York, NY, USA, 2008.
6. Shao, L.; Hua, W.; Dai, N.; Tong, M.; Cheng, M. Mathematical modeling of a twelve-phase flux-switching permanent-magnet machine for wind power generation. *IEEE Trans. Ind. Electron.* **2016**, *63*, 504–516. [[CrossRef](#)]
7. Gao, Y.; Qu, R.; Li, D.; Li, J.; Zhou, G. Consequent-pole flux-reversal permanent-magnet machine for electric vehicle propulsion. *IEEE Trans. Appl. Supercond.* **2016**, *26*, 5200105. [[CrossRef](#)]
8. Zhao, J.; Yan, Y.; Li, B.; Liu, X.; Chen, Z. Influence of Different Rotor Teeth Shapes on the Performance of Flux Switching Permanent Magnet Machines Used for Electric Vehicles. *Energies* **2014**, *7*, 8056–8075. [[CrossRef](#)]
9. Zhang, W.; Liang, X.; Lin, M.; Hao, L.; Li, N. Design and analysis of novel hybrid-excited axial field flux-switching permanent magnet machines. *IEEE Trans. Appl. Supercond.* **2016**, *26*, 1.
10. Hua, W.; Zhang, G.; Cheng, M. Investigation and design of a highpower flux-switching permanent magnet machine for hybrid electric vehicles. *IEEE Trans. Magn.* **2015**, *51*, 8201805.
11. Chen, H.; At-Ahmed, N.; Machmoum, M.; Zam, M.E.H. Modeling and vector control of marine current energy conversion system based on doubly salient permanent magnet generator. *IEEE Trans. Sustain. Energy* **2015**, *7*, 409–418. [[CrossRef](#)]

12. Liao, Y.; Liang, F.; Lipo, T.A. A novel permanent magnet motor with Doubly Salient structure. *IEEE Trans. Ind. Appl.* **1995**, *31*, 1069–1078. [[CrossRef](#)]
13. Zhu, S.; Cheng, M.; Dong, J.; Du, J. Core loss analysis and calculation of stator permanent-magnet machine considering DC-biased magnetic induction. *IEEE Trans. Ind. Electron.* **2014**, *61*, 5203–5212. [[CrossRef](#)]
14. Chau, K.T.; Sun, Q.; Fan, Y.; Cheng, M. Torque ripple minimization of doubly salient permanent magnet motors. *IEEE Trans. Energy Convers.* **2005**, *20*, 352–358. [[CrossRef](#)]
15. Xu, W.; He, M. Novel 6/7 stator/rotor hybrid excitation doubly salient permanent magnet machine. *IEEE Trans. Magn.* **2016**, *52*, 1–5. [[CrossRef](#)]
16. Yu, L.; Zhang, Z.; Chen, Z.; Yan, Y. Analysis and verification of the doubly salient brushless DC generator for automobile auxiliary power unit application. *IEEE Trans. Ind. Electron.* **2014**, *61*, 6655–6663. [[CrossRef](#)]
17. Wang, Y.; Zhang, Z.; Yu, L. Investigation of a variable-speed operating doubly salient brushless generator for automobile on-board generation application. *IEEE Trans. Magn.* **2015**, *51*, 1–4. [[CrossRef](#)]
18. Gong, Y.; Chau, K.T.; Jiang, J.Z.; Yu, C. Design of doubly salient permanent magnet motors with minimum torque ripple. *IEEE Trans. Magn.* **2009**, *45*, 4704–4707. [[CrossRef](#)]
19. Zhang, Z.; Yan, Y.; Tao, Y. A new topology of low speed doubly salient brushless DC generator for wind power generation. *IEEE Trans. Magn.* **2012**, *48*, 1227–1233. [[CrossRef](#)]
20. Wu, Z.Z.; Zhu, Z.Q.; Shi, J.T. Novel doubly salient permanent magnet machines with partitioned stator and iron pieces rotor. *IEEE Trans. Magn.* **2015**, *51*, 8105212. [[CrossRef](#)]
21. Sriwannarat, W.; Khunkitti, P.; Janon, A.; Siritaratiwat, A. An Improvement of Magnetic Flux Linkage in Electrical Generator using the novel Permanent Magnet Arrangement. *Acta Phys. Pol. A* **2005**, *133*, 642–644. [[CrossRef](#)]
22. Zhang, J.; Cheng, M.; Xiaoyong, Z. A novel three-phase doubly salient permanent magnet generator. In *2015 International Conference on Electrical Machines and Systems; ICEMS: Nanjing, China, 2005; Volume 1*, pp. 407–411.



© 2019 by the authors. Licensee MDPI, Basel, Switzerland. This article is an open access article distributed under the terms and conditions of the Creative Commons Attribution (CC BY) license (<http://creativecommons.org/licenses/by/4.0/>).